Journal of Materials Chemistry A

Accepted Manuscript

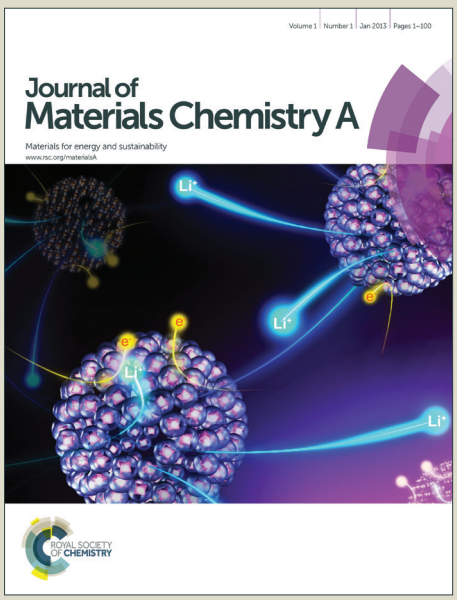

ROYAL SOCIETY OF CHEMISTRY

www.rsc.org/materialsA

Journal Name

RSCPublishing

ARTICLE

Metal-Organic Frameworks deposition on dealloyed substrates

Cite this: DOI: 10.1039/x0xx00000x

Nicolò Campagnol,[a] Ivo Stassen,[b] Koen Binnemans,[c] Dirk E. De Vos,[b] and Jan Fransaer[a*]

Received ooth January 2012,
Accepted ooth January 2012

DOI: 10.1039/x0xx00000x

www.rsc.org/

The functionalization of surfaces to obtain high specific surface areas is important for catalysis, energy storage and sensing. The two main approaches to obtain porous surfaces are the deposition of porous materials, like Metal-Organic Frameworks (MOFs), and the modification of the substrates, for example by dealloying. MOF layers have higher specific surface areas than dealloyed structures, but they are easily damaged by external forces. In this work we report on the combination of dealloying and MOF deposition. The functionalised surfaces have a much higher specific surface area (*circa* 7000 m^2/m^2) than the simple sum of the specific area of a MOF layer and a dealloyed one. Moreover, the MOF crystals are protected by the dealloyed structures and are not easily removed by an external force. The presence of the metal scaffold may also enable fast heat exchange with the MOF, which is important for the use of these structures in e.g. adsorption rotors.

Introduction

Metal-Organic Frameworks (MOFs) are a novel class of coordination polymers famous for their high surface area and tuneable porosity. They are composed of metal, or metal oxide centres of coordination connected by organic bridges, termed linkers. A virtually infinite number of these compounds can be synthesised thanks to the availability of many different linkers and metals. In fact, more than 20,000 different MOF structures have been reported within the last decade.[1] Many possible applications have been proposed for these materials, among them: gas sorption,[2] sensing,[3] and energy storage,[4] and various companies are already working to bring to the market MOFs for the transport, textile and respiratory devices industries.[5]

Shaping these novel materials is challenging but often indispensable for certain applications where porous materials are already commonly used.[6-8] Many methods have been proposed and tested to make MOF films, among which growth/deposition from solvothermal mother solutions, microwave-induced thermal deposition, layer-by-layer or liquid phase epitaxy of SURMOFs, electrochemical synthesis, and evaporation induced crystallization.[7, 9]

The anodic electrochemical technique is based on the electrochemical dissolution of metal ions in a solution containing the linker needed to make the MOF. It was invented by Mueller et al.[10] to synthesise MOFs powders in large quantities avoiding the use of metal salts. Starting from this work, our group developed the anodic electrodeposition method to obtain MOF coatings.[11] Li and Dinca reported another technique to synthesise MOF layers electrochemically, starting from a solution containing both the linker and the metal salt. This technique is based on the deprotonation the linker at the cathode, where the deposition happens.[12, 13] The anodic method was applied to several MOFs and substrates,[14-21] and special attention was given to the mechanical adhesion of the layers. The adhesion is important both under external perturbation when the layer is already formed,[17] and during its formation.[22] In the first case, the result of an external load on the surface can be more or less destructive for the layer depending on the MOF, and possibly the synthesis method,[20] and at the point where a scratching body passes, no coating is left in any case.[17] On the other hand, we recently showed that adhesion problem also arise in the synthesis step. During an anodic MOF deposition process, the porous layer grows at the MOF-solution interphase while fed by metal ions produced from the substrate, and this process creates voids at the MOF-substrate interphase. These voids and the compressive stresses that arise in these MOF layers during anodic synthesis might lead to an 'undercut' of the crystals and consequent detachment of part of the layers.[22] In both cases the functional part (the MOF) is lost, and the parts of the surface previously coated become inactive for applications like catalysis or sensing.

Alloys are formed by two or more metallic elements and can be affected by galvanic corrosion. When an electrolyte is present (*e.g.* salt water on brass or bronze) the more "noble" regions of the surface act as cathode and the less noble ones as anode. Due to this, the anodic regions dissolve in solution as ions. If pure metals or alloys composed of only one phase are

used, the less noble areas can be inclusions or grain boundaries, but in multiphase alloys the nobility is determined by the chemical composition.[23] Due either to galvanic corrosion or to an external potential applied to the sample, the least noble metal atoms go in solution as ions, leaving the noblest ones on the surface. The "noble" adatoms left on the surface migrate to form clusters which are unaffected by the potential applied and form a porous structure during the layer-by-layer removal of the remaining alloy matrix.[23] Due to their high surface area and conductivity, dealloyed structures have been used for several applications, e.g. catalysis and energy storage.[24]

This works aims to merge two techniques, *viz.* MOF electrodeposition and dealloying. The obtained coatings are expected to have the mechanical resistance of a dealloyed surface, together with the high specific surface area typical of MOF coatings. MOF crystals may grow inside the voids created by the leaching of the least noble phase of the alloy, allowing a high loading of MOF crystals without encountering problems connected with thick fragile layers. Moreover, the dealloyed structure may avoid the phenomenon of the undercut due to the fact that only one of the phases goes in solution, leaving the second (more noble) phase in place to provide adhesion with the MOF layer. The dealloyed structure also provides a physical containment to the MOF crystals which protects the layers from mechanical forces which could still remove the top surface MOF layer (as already seen with MOF layers on flat surfaces) but not the MOF crystals inside the dealloyed structure.

Experimental

Alloy preparation

Ag-Cu alloys were prepared in an induction furnace (Manfredi-Saed Neutor Digital) by melting the selected ratios of Ag (99% pure) and Cu (99% pure) and spin casting the liquid metal either in a rod-shaped or in a plate-shaped steel die. The rods (9 cm long, and 0.8 cm in diameter) were then processed in three ways, as shown in **Figure 2**. In the first case, they were cold-rolled to obtain foils with crystals elongated in the rolling direction (parallel to the surface) (a). Alternatively, the rods were sliced directly after casting, obtaining samples with equi-axial grains (b), or drawn to a smaller diameter and sliced, obtaining coin-shaped samples with grains oriented perpendicularly to the surface (c). The composition of the cast samples was routinely checked with EDX (FEI XL-30). Another technique to obtain grains oriented perpendicularly to the surface is dip-coating. For this work a copper plate was rapidly dipped in the molten metal with the right composition. A thin layer of the alloy solidifies on the plate, and the homogeneity and thickness of the layer depend on the immersion time, dipping speed and bath temperature.

Dealloying

The samples with different grain orientations were subsequently dealloyed either chemically or electrochemically. Chemical dealloying is often more time consuming in comparison to the electrochemical method, but sometimes the resulting layers have different properties.[25] A possibility to chemically dealloy copper from an Ag-Cu alloy is to make use of its stable oxidation state in different solutions, for example acetonitrile (ACN). The divalent Cu^{2+} is the most stable state in water, but through the addition of few vol% of acetonitrile the most stable state becomes Cu^{+}.[26] A solution containing 25 vol% ACN (Acros Organics, 99.8%) in demi water and 30 g/L $CuSO_4$ (0.18 M, Sigma-Aldrich) was used to chemically dealloy the samples: the Cu^{2+} ions oxidise metallic copper to Cu^{+} leaving behind a silver based porous structure.[26]
Electrochemical dealloying was done similarly to what has been reported by Li et al.[27]. The bath used was a 30 g/L (0.18 M) $CuSO_4$ aqueous solution and, except where stated otherwise, 0.15 V vs a copper counter electrode was applied for 3 h with an EG&G 273 potentiostat. The dealloyed samples were checked with XRD (Seifert 3003), and with optical (Leica DMILM) and electron (XL-30, and Focus Ion Beam equipped FIB-NanoSEM FEI Nova 600 Nanolab) microscopes.

MOF anodic electrodeposition

The dealloyed samples were used as starting substrates for the anodic electrodeposition synthesis of MOFs. The solution used is based on the work of Van Assche et al.[28] and consists of 25 vol% demi water in pure ethanol, with 16 g/L of trimesic acid (H_3BTC, 98% pure, ABCR). The electrodeposition was run at room temperature, in a three-electrodes set-up using platinum as counter electrode, a home-made Ag/AgCl reference electrode, and the dealloyed samples as working electrodes. 4 V vs reference were applied for 20 minutes with an EG&G 273 potentiostat. The obtained samples were checked with SEM (XL-30, FIB-NanoSEM) and XRD.

Porosimetry tests

The specific surface area of the samples, in m^2/m^2, was calculated from the krypton adsorption isotherms measured at 77 K using a Micromeritics 3Flex 3500 physisorption instrument. The samples were degassed before measurement at 423 K under vacuum (10^{-2} mbar) for 1 h. Gas uptake equilibria were measured between 10^{-5} and 2.15 mbar (deposition saturation pressure, $P_{0,solid}$). As adsorption of liquid-like multilayers is assumed in the BET theory, the extrapolated condensation saturation pressure of the supercooled liquid ($P_{0,liquid}$ ~ 3.3 mbar) was used as P_0 value for isotherm plotting and BET
calculations. The BET method was applied in the region between 0.0005 and 0.10 P/P_0 for the MOF containing samples

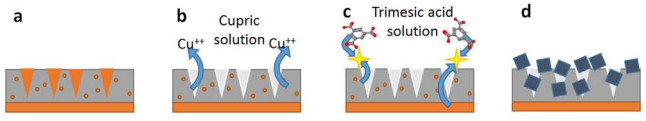

Figure 1: Scheme representing the samples preparation: the chosen alloy composition is cast or dip coated to obtain a substrate (a), this substrate is dealloyed in a cupric bath yielding to a porous silver rich layer (b), the sample is further dissolved in a solution containing trimesic acid where the copper ions released react with the ligand (c) and precipitate as MOF crystals (d).

and in the region between 0.10 and 0.35 P/P_0 for the samples that were only dealloyed. An adsorptive cross-sectional area of 0.210 nm² was assumed for krypton atoms. Twelve samples with composition $Ag_{15}Cu_{85}$ (circa 30 mm^2 each) with grains oriented perpendicular to the surface were dealloyed for 3 h at 0.15 V vs copper in a cupric bath; six of them were then used to electrodeposit MOF. The same solution and setting were used to synthesise MOF layers on six copper plates of similar dimensions. The three groups of samples have been used to measure the krypton adsorption capacity obtainable for each synthesis method. The area of the samples was limited by the use of lacquer during the depositions and then carefully measured with an optical microscope coupled with image analysing software (Imagej).

Results and discussion

The scheme of the sample preparation is reported in **Figure 1**: the substrates were obtained by casting or dip coating, then dealloyed and finally deposited with MOF to obtain composite dealloyed+MOF layers.

Since copper-based MOFs are the most studied for electrochemical synthesis,[17, 22, 28] copper was chosen as least noble element of the alloy. In order to have dissolution of this element in the form of ions in an electrolyte, a more noble metal has to be combined with it. Not many metals are nobler than copper, and the cheapest and most easily available of this group is silver. Ag-Cu is a good example of a eutectic alloy without intermetallic phases. In fact, Ag and Cu are almost completely immiscible at room temperature and therefore the obtained microstructure is composed of grains of copper-rich and silver-rich phases.[29]

Except when the eutectic composition ($Ag_{60}Cu_{40}$) is chosen, three phases are present in the cast Ag-Cu samples. Taking as example $Ag_{15}Cu_{85}$, the first phase to nucleate upon cooling is a copper rich phase (α), which contains up to 5 at% Ag. This phase is very important for this work because the microstructure of the final layer depends on the orientation and dimensions of these crystals. According to the Ag-Cu phase diagram, at 779 °C two additional phases nucleate forming the matrix of the microstructure: an α phase richer in Ag in comparison to the already nucleated one (8 at%), which will be called α′, and a β phase consisting of 91 at% silver. The amount of the three phases is not equal and depends on the composition of the alloy and on the cooling procedure, see XRD in **S3**. In the experiments reported in this work, the samples were not quenched but the cooling was relatively fast; therefore the grains are of the micron size and the amount of phase α′ is relatively small in comparison to the other two. Three compositions were studied in this work: $Ag_{15}Cu_{85}$, $Ag_{30}Cu_{70}$, and $Ag_{45}Cu_{55}$. Upon dealloying, the α phase dissolves, leaving micron-sized voids containing a certain amount of nanometric silver-rich phase. The α′ and β phases are also affected by the dealloying: small holes (less than a µm in size) can be seen in the matrix due to the copper leached from these phases.

Different compositions have different ratios of α and β phases, leading to a prevalence of the scaffold with small voids for the silver-rich samples and to a thinner structure with big voids for the samples with lower amount of silver. In the **S1** and **S2** more information on the different phases, the dealloying mechanism and the effect of the chemical compositions can be found.

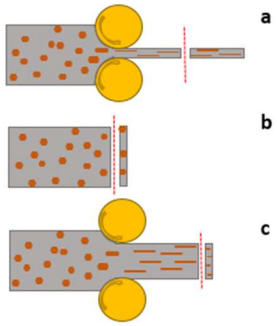

Figure 2: Scheme of the preparation of the alloy samples: (a) rolling and cutting (grains parallel to the surface), (b) slicing after casting (equi-axial grains), and (c) rolling and slicing (grains perpendicular to the surface).

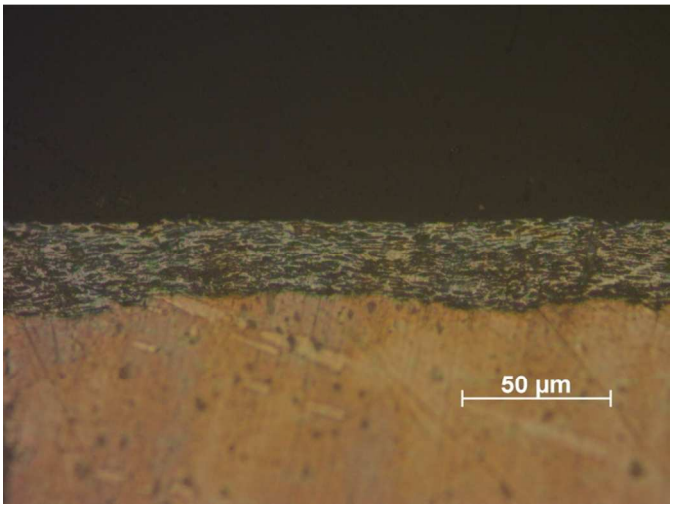

Figure 3: Optical cross-section of a $Ag_{15}Cu_{85}$ sample obtained by rolling, dealloyed electrochemically in cupric solution.

Dealloyed biphasic alloys with crystals in the micron range are less studied for applications than monophasic ones.[23, 27, 30] The reason is that the obtained dealloyed structures are not completely nanometric and therefore have lower surface areas. Nevertheless, voids in the micrometre range are more suitable for this work than nanometric ones, as after MOF growth, micron sized voids offer space for fluids (liquid or gasses) to rapidly diffuse in the structure. This is the reason why the $Ag_{15}Cu_{85}$ composition has been preferred for this work.

The easiest way to produce a metal sheet is to cast a plate and roll it, see **Figure 2**. This technique leads to a crystal structure made out of long flat grains parallel to the surface. Unfortunately, upon dealloying, grains oriented parallel to the surface give rise to voids that are difficult to access from the surface (**Figure 3** and **S2**) while grains oriented perpendicularly lead to deep holes connected to the surface, easily accessible for a solvent or a gas**.** Non-oriented microstructures can be obtained by avoiding thermal gradients during solidification and post-deformation of the cast samples. For example, by slicing the alloy rods after casting, or by using a steel die shaped as a plate to rapidly solidify a sample. Similarly to what

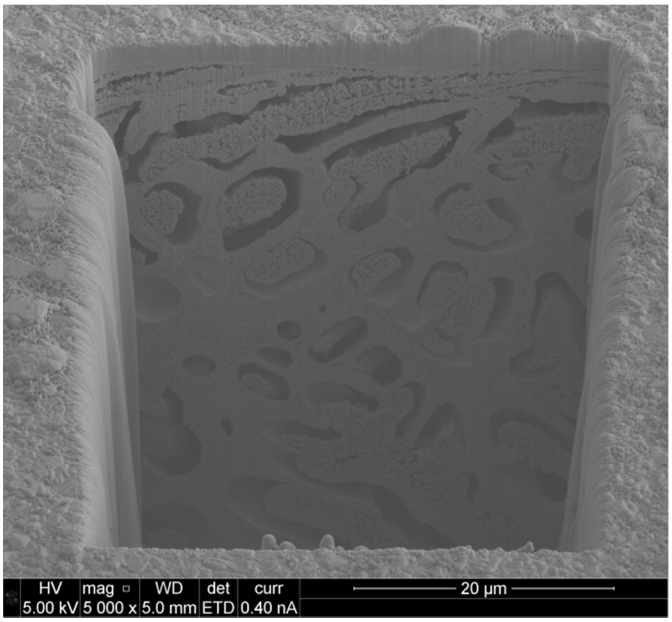

Figure 4: SEM-FIB cross-section of a drawn Ag15Cu85 sample after chemically dealloying.

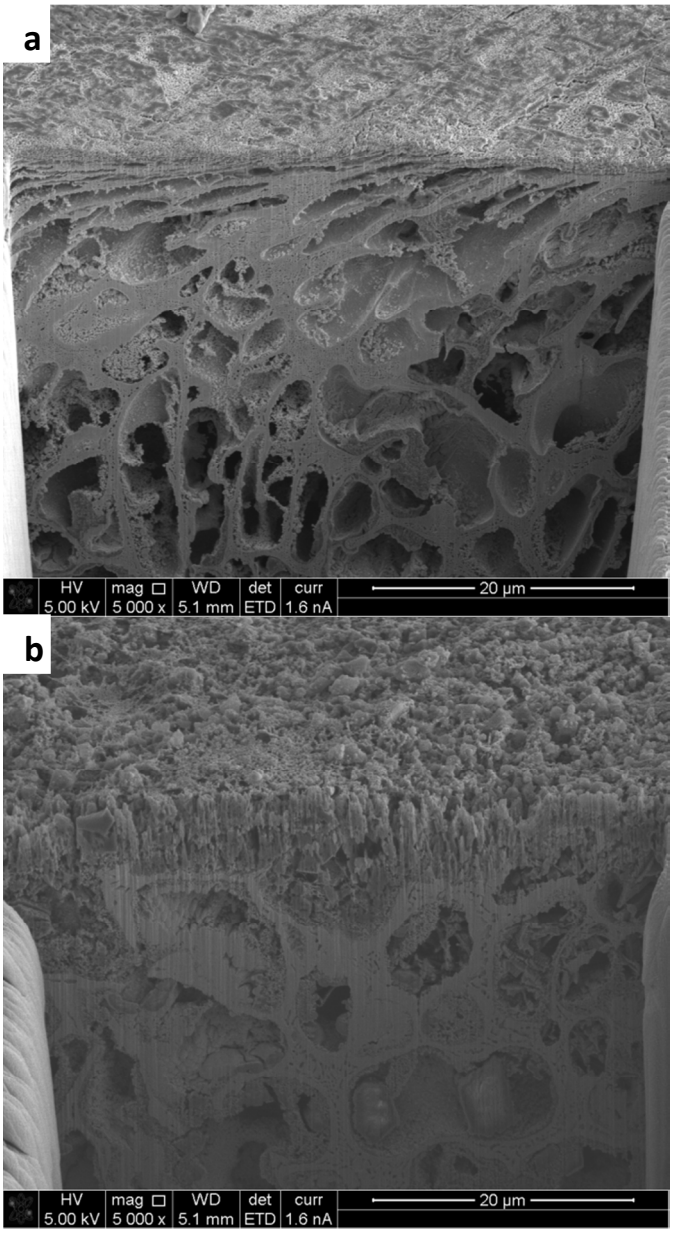

Figure 5: SEM-FIB cross-section of a drawn and sliced $Ag_{15}Cu_{85}$ sample electrochemically dealloyed (a) and converted into MOF (b).

was stated above, orienting the grains perpendicularly to the surface can be done by a directional solidification or by deformation. The first can be obtained by dip-coating, for example by immersing a copper plate in a Ag-Cu melt of the right composition. The copper surface acts as seed for the nucleation, while the rest of the plate drains the heat, providing a directional thermal gradient perpendicular to its surface. The second method is based on drawing and slicing the rods obtaining coins with grains oriented perpendicularly to the surface. Dip-coating would be the most advisable for industrial applications since it is fast and can be applied to a wide variety of substrates (any metal with good heat conductivity and relatively high melting point), but with the set-up available for this work only thin layers of Ag-Cu alloy could be obtained (see **S4**). The choice of the substrate for the dip-coating and the dealloying conditions influence the resulting porous layer: for example copper as substrate gives a good adherence of the Ag-Cu alloy, but it is easy to undercut the silver-rich porous structure once the dealloying front arrives at the interphase between substrate and dip-coated layer. With the drawing and slicing technique the samples are more limited in dimensions (except in thickness) but the method is more practical for a scientific investigation, and this is the reason why for this paper this technique was preferred.

As previously stated, the dealloying step can be done chemically or electrochemically, and the resulting microstructures differ depending on the method used. Electrochemical dealloying was normally run in a two electrodes set-up, but to better compare samples with different grain orientations, one sample per type was dealloyed in a three electrode set-up, applying 0.25 V vs Ag/AgCl reference electrode (corresponding to 0.15 V vs copper) for 3 h. It was observed that the obtained dealloyed structures extended for different depths inside the samples, see **S6**. Grains oriented perpendicularly to the surface are more prone to leaching in the solution and the dealloyed layers obtained with these samples measure circa 80 µm in thickness. On the other hand, grains oriented parallel to the surface are less affected by the leaching process, and the obtained layers are thinner (30 µm). Layers obtained from samples with equi-axial grains show intermediate values, around 45 µm. From the top view, samples obtained by drawing and slicing or by dip-coating show deep voids, while dealloyed samples with grains parallel to the surface show areas with nano-porous silver-rich phases, but no deep voids, see **S8**. The change in phase distribution can be observed also from the XRD patterns of the samples: after dealloying the peaks corresponding to the copper phase

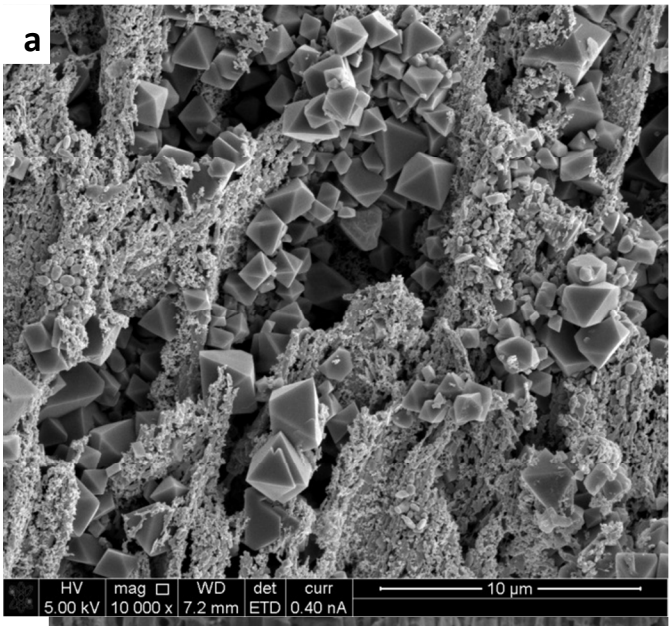

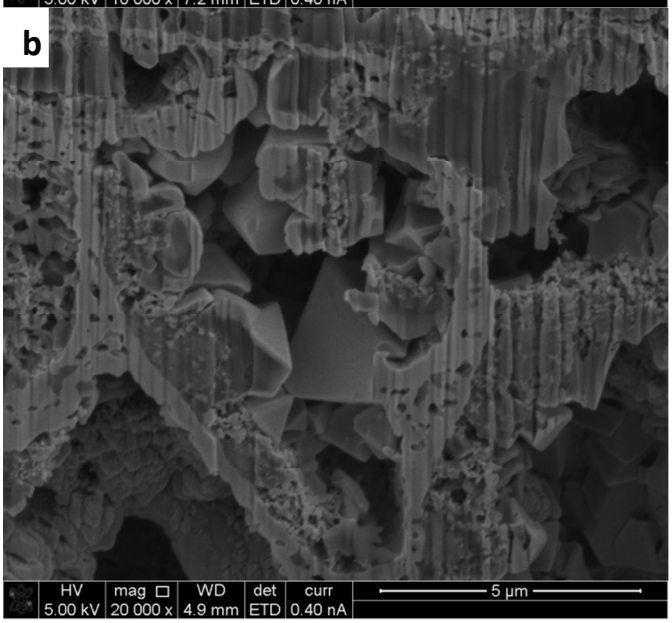

Figure 6: SEM-FIB images of a drawn and sliced $Ag_{15}Cu_{85}$ sample electrochemically dealloyed and converted into MOF. Top view of the surface (a) and detail of the cross-section (b).

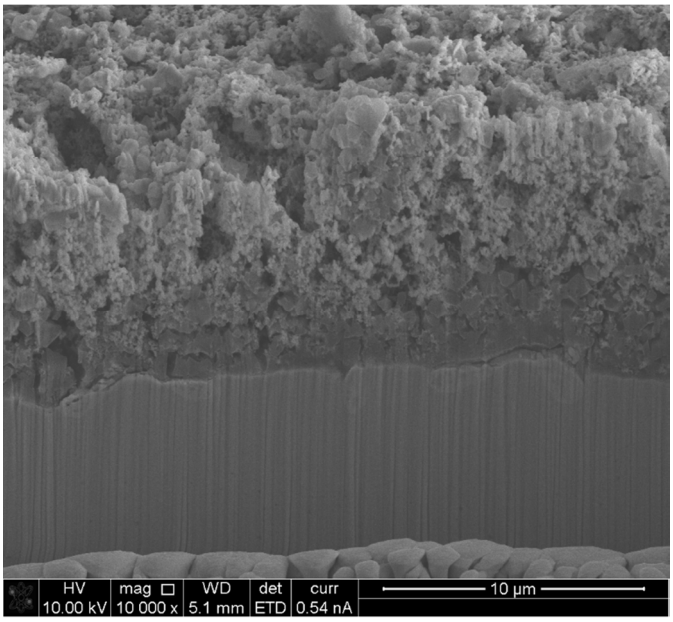

Figure 7: SEM-FIB cross-section of a dip coated $Ag_{15}Cu_{85}$ sample after electrochemical dealloying in a cupric solution and MOF deposition.

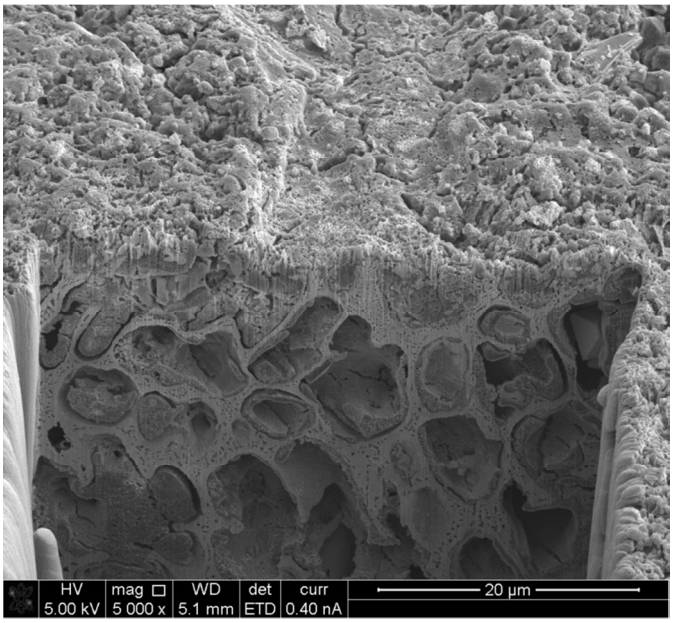

Figure 8: SEM-FIB cross-section of a drawn $Ag_{15}Cu_{85}$ sample electrochemically dealloyed, converted into MOF and scratched with a diamond tip.

decrease in intensity, while those corresponding to the silver one become more prominent, see **S3**. Chemical dealloying was applied on a sample with grains oriented perpendicularly to the surface. From the cross-section (**Figure 4**) large amounts of the nanometre-sized silver-rich phase are still left inside the micron-sized voids. A rapid screening (**see S9)** showed that to obtain a dealloyed structure of circa 50 µm depth with the solution used, it is necessary to leave the samples for 24 h in the liquid.

MOF electrodeposition has been achieved with all the dealloyed samples with a starting composition of $Ag_{15}Cu_{85}$, see **Figure** 5 and the XRD patterns in S3. The same settings were used for all samples: 4 V vs Ag/AgCl applied for 20 min in a solution containing the linker. In the dealloyed samples, the copper ions are released from the bulk of the alloy, where the dealloying process did not reach, and from the grains already partially dissolved. The nucleation and growth happen on the top surface and inside the voids, sometimes filling them completely, see **Figure 6**. This process avoids the problem of MOF film detachments observed for flat substrates[22] since the crystals are mechanically confined inside the voids and anchored to the silver scaffold, which does not dissolve during MOF synthesis. The MOF electrodeposition step can be well observed comparing the pictures of **Figure 5** and **Figure 7**. The

first picture of **Figure 5** shows a sample with vertically oriented grains after electrochemical dealloying, featuring large empty voids which in many cases reach the surface, only partially occupied by a nanostructured silver-rich phase; in contrast, on the following pictures, the voids of the samples obtained by drawing and by dip-coating are almost
completely filled with the MOF phase. The sharp edges characteristic of Cu-BTC crystals are sometimes difficult to distinguish in the filled holes, but are recognisable on the top surface which is also covered by these crystals. The XRD patterns confirm the presence of MOF, but the patterns are not as sharp as those of pure HKUST-1 on copper flat substrates. Chemically dealloyed samples have less space inside the voids for hosting MOF crystals (see **S10**), but still show an effective incorporation of the crystals in the dealloyed structure.

One of the aims of this work was to produce a layer which would be less affected by external perturbations. This result has been achieved and can be appreciated from **Figure 8**, which shows an electrochemically dealloyed sample electrodeposited with MOF, after scratching with a diamond tip. The MOF crystals on the top surface are dragged away by the diamond tip, but those below, being protected by the metallic porous architecture, are not affected. More information can be found in the **S11** and **S12** showing the effect of even deeper scratches.

Figure 9 compares the amounts of krypton adsorbed by an electrochemically dealloyed surface, a MOF layer, and a MOF layer deposited on a dealloyed surface. From the amount of krypton adsorbed, it was calculated the specific surface area per unit of area (in m^2/m^2) of the samples. The specific surface of the dealloyed samples is already very high, 470 m^2/m^2, but still much lower than that of a copper plate covered by MOF, 2433 m^2/m^2, which demonstrates the high porosity of these materials. When the two techniques are combined, *i.e.* when a MOF layer is grown from a dealloyed surface, the surface area further increases by a factor of 2.85, reaching almost 7000 m^2/m^2 (6920 m^2/m^2). As expected, this is the result of a combination of the dealloyed surface area, which gives the slight tilt to the adsorption curve, and the presence of circa two and a half times the amount of MOF crystals in comparison to a flat surface. Using the density of HKUST-1 (1.22 g/cm^3)[31] and BET area (692 m^2/g, measured with nitrogen)[31] the amount of MOF on pure copper substrates and on the Ag-Cu dealloyed substrates was estimated as 0.0035 mg/mm^2 and 0.01 mg/mm^2 respectively. As a check, the thickness of 2.9 µm for the MOF on the pure copper substrate samples was also estimated from these measurements. This thickness was verified from the FIB cross-section of one of the plates used for the measurements.

Conclusions

In this work the possibility of combining dealloying and electrochemical deposition of MOFs was demonstrated, to obtain layers with very high porosity and good mechanical properties. Different structures have been obtained with a silver-copper alloy, changing the composition, cooling and post-synthesis deformation. Electrochemical dealloying was used for most of the experiments due to the simplicity and speed. Nevertheless, also a chemical dealloying route has been explored, showing that a solution containing Cu^{2+} ions and acetonitrile can preferentially dissolve copper, forming a porous structure similar to those obtained electrochemically.

The archetypal MOF HKUST-1 was synthesised electrochemically using dealloyed structures as precursors. Copper(II) ions diffuse from the bulk of the samples and MOF crystals form both inside the voids made during the dealloying step, and on the top surface of the samples. The anchoring to the silver-rich scaffold avoids the risk of detachment during synthesis observed using copper plates as substrates, and the scaffold acts as a protection for the MOF crystals from external forces. When scratched with a diamond tip, the top surface is heavily damaged and the MOF layer is locally removed, but the lower layers remain full of MOF crystals and the sample therefore retains its large surface area. The specific surface area in m^2/m^2 was measured with krypton porosimetry. The surface area of the MOF layers grown on dealloyed samples is 2.85 times larger than that of a MOF layer grown on a flat copper substrate under the same synthesis conditions. This improvement may have a direct effect in the use of these layers for catalysis and moreover, it can be speculated that the close proximity of MOF and metal can be beneficial for applications where fast absorption and desorption of gasses by the MOF layers is accompanied by the uptake or release of heat.

Acknowledgements

The authors thank the IWT for support in the SBO-project MOFShape. The authors thank the Hercules 3 ZW09-09 project for the FIB-NanoSEM pictures.

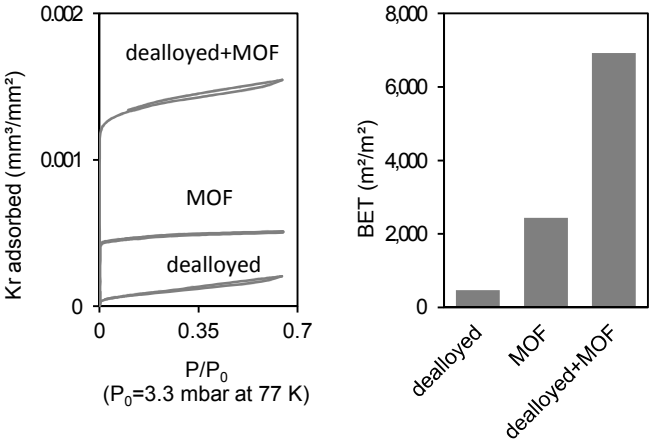

Figure 9: Comparison between krypton porosimetry measurements, in mm^3 of Kr adsorbed divided by the projected area of the samples in mm^2 (a) and BET area divided by the projected area (b) of a dealloyed $Ag_{15}Cu_{85}$ sample, a HKUST-1 layer on a flat copper substrate, and a $Ag_{15}Cu_{85}$ dealloyed sample deposited with HKUST-1.

Notes and references

[a]*Department of Materials Engineering (MTM), KU Leuven, Kasteelpark Arenberg 44, B-3001 Leuven, Belgium. E-mail: Jan.Fransaer@mtm.kuleuven.be*

[b]*Centre for Surface Chemistry and Catalysis (COK), KU Leuven, Kasteelpark Arenberg 23, B-3001 Leuven, Belgium.*

[c]*Department of Chemistry, KU Leuven, Celestijnenlaan 200F, B-3001 Leuven, Belgium*

† Electronic Supplementary Information (ESI) available: SEM cross-section of the dealloying process, influence of the composition on the microstructure, cross-section and picture of dip coated samples, optical cross-section of dealloyed samples with different grain orientation, SEM top view of dealloyed surfaces, time evolution of chemical dealloying, SEM-FIB images of scratched samples. See DOI: 10.1039/b000000x/

1. H. Furukawa, K. E. Cordova, M. O'Keeffe and O. M. Yaghi, *Science*, 2013, **341**, 1230444.
2. J. Canivet, A. Fateeva, Y. Guo, B. Coasne and D. Farrusseng, *Chemical Society Reviews*, 2014, **43**, 5594-5617.
3. Z. Hu, B. J. Deibert and J. Li, *Chemical Society Reviews*, 2014, **43**, 5815-5840.
4. A. Morozan and F. Jaouen, *Energy and Environmental Science*, 2012, **5**, 9269-9290.
5. P. Silva, S. M. Vilela, J. P. Tomé and F. A. A. Paz, *Chemical Society Reviews*, 2015.
6. P. Falcaro, R. Ricco, C. M. Doherty, K. Liang, A. J. Hill and M. J. Styles, *Chemical Society Reviews*, 2014, **43**, 5513-5560.
7. O. Shekhah, J. Liu, R. A. Fischer and C. Woll, *Chemical Society Reviews*, 2011, **40**, 1081-1106.
8. N. Rangnekar, N. Mittal, B. Elyassi, J. Caro and M. Tsapatsis, *Chemical Society Reviews*, 2015.
9. A. Betard and R. A. Fischer, *Chemical Reviews*, 2012, **112**, 1055-1083.
10. U. Mueller, M. Schubert, F. Teich, H. Puetter, K. Schierle-Arndta and J. Pastréa, *Journal of Materials Chemistry*, 2006, **16**, 626-636.
11. R. Ameloot, L. Stappers, J. Fransaer, L. Alaerts, B. F. Sels and D. E. De Vos, *Chemistry of Materials*, 2009, **21**, 2580-2582.
12. M. Li and M. Dinca, *Journal of the American Chemical Society*, 2011, **133**, 12926-12929.
13. H. Liu, H. Wang, T. Chu, M. Yu and Y. Yang, *Journal of Materials Chemistry C*, 2014, **2**, 8683-8690.
14. N. N. Adarsh, M. M. Dîrtu, A. D. Naik, A. F. Léonard, N. Campagnol, K. Robeyns, J. Snauwaert, J. Fransaer, B. L. Su and Y. Garcia, *Journal*, 2015, n/a.
15. N. Campagnol, E. R. Souza, D. E. De Vos, K. Binnemans and J. Fransaer, *Chemical Communications*, 2014, **50**, 12545-12547.
16. N. Campagnol, T. Van Assche, T. Boudewijns, J. Denayer, K. Binnemans, D. De Vos and J. Fransaer, *Journal of Materials Chemistry A*, 2013, **1**, 5827-5830.
17. B. Van de Voorde, R. Ameloot, I. Stassen, M. Everaert, D. De Vos and J.-C. Tan, *Journal of Materials Chemistry C*, 2013, **1**, 7716-7724.
18. K.-Y. Cheng, J.-C. Wang, C.-Y. Lin, W.-R. Lin, Y.-A. Chen, F.-J. Tsai, Y.-C. Chuang, G.-Y. Lin, C.-W. Ni, Y.-T. Zeng and M.-L. Ho, *Dalton Transactions*, 2014, **43**, 6536-6547.
19. H. Yang, H. Du, L. Zhang, Z. Liang and W. Li, *International Journal of Electrochemical Science*, 2015, **10**, 1420-1433.
20. I. Stassen, M. J. Styles, T. R. Van Assche, N. Campagnol, J. Fransaer, J. F. Denayer, J.-C. Tan, P. Falcaro, D. E. De Vos and R. P. Ameloot, *Chemistry of Materials*, 2015.
21. W. Li, J. Lu, S. Gao, Q. Li and R. Cao, *Journal of Materials Chemistry A*, 2014.
22. N. Campagnol, T. Van Assche, L. Stappers, J. F. M. Denayer, K. Binnemans, D. E. De Vos and J. Fransaer, *ECS Transactions*, 2014, **61**, 25-40.
23. J. Erlebacher, M. J. Aziz, A. Karma, N. Dimitrov and K. Sieradzki, *Nature*, 2001, **410**, 450-453.
24. H. J. Qiu, H.-T. Xu, L. Liu and Y. Wang, *Nanoscale*, 2015, **7**, 386-400.
25. K. L. Fow, M. Ganapathi, I. Stassen, J. Fransaer, K. Binnemans and D. E. De Vos, *Chemical Communications*, 2013, **49**, 8498-8500.
26. A. J. Parker, *Proceedings of the Royal Australian Chemical Institute*, 1972, **39**, 163-170.
27. G. Li, X. Song, Z. Sun, S. Yang, B. Ding, S. Yang, Z. Yang and F. Wang, *Solid State Sciences*, 2011, **13**, 1379-1384.
28. T. R. C. Van Assche, G. Desmet, R. Ameloot, D. E. De Vos, H. Terryn and J. F. M. Denayer, *Microporous and Mesoporous Materials*, 2012, **158**, 209-213.
29. J. R. Davis, *Copper and copper alloys*, ASM international, 2001.
30. Q. Chen and K. Sieradzki, *Nature Materials*, 2013, **12**, 1102-1106.
31. S. S. Y. Chui, S. M.-F. Lo, J. P. H. Charmant, A. G. Orpen and I. D. Williams, *Science*, 1999, **283**, 1148-1150.

Visual abstract

Dealloyed structures are used as substrate to grow MOFs electrochemically. The resulting layers have high surface area and are resistant to scratches.